Predicting *in vivo* concentrations of dietary hop phytoestrogens by physiologically based kinetic modeling

Maja Stevanoska [a], Karsten Beekmann [b], Ans Punt [b], Shana J. Sturla [a], Georg Aichinger [a],*

[a] *Department of Health Sciences and Technology, ETH Zurich, Switzerland*
[b] *Wageningen Food Safety Research (WFSR), Netherlands*

ARTICLE INFO

ABSTRACT

Hop extracts containing prenylated polyphenols such as 8-prenylnaringenin (8-PN) and its precursor iso-xanthohumol (iXN) are popular among women seeking natural alternatives to hormone therapy for post-menopausal symptoms. Due to structural similarities with estrogens, these compounds act as estrogen receptor agonists. Especially 8-PN, described as the most potent phytoestrogen known to date, poses a potential risk for endocrine disruption. Therefore, its use as a hormone replacement raises concerns for human health. However, a significant challenge in assessing the potential endocrine-disruptive effects of hop polyphenols is the lack of data on their toxicokinetics. Particularly, information on *in vivo* concentrations in target tissues is lacking. To address this gap, we developed a physiologically based kinetic (PBK) model tailored to female physiology. The model was used to predict the levels of hop polyphenols in human blood and target tissues under realistic exposure scenarios. The predictions suggest that iXN and 8-PN concentrations in target tissues reach the low nanomolar range after dietary supplementation. This study enhances our understanding of internal concentrations of iXN and 8-PN after dietary consumption and is of direct applicability for respective risk assessment.

1. Introduction

Although hormone therapy is a primary recommended treatment for early menopausal symptoms (Pinkerton, 2020), the associated increased risk of breast cancer (Narod, 2011) has led many women to seek natural alternatives (Beral et al., 2003). Supplements derived from female hop flowers, which are rich in prenylated polyphenols, including chalcones and flavonoids are a popular choice among postmenopausal women to alleviate postmenopausal symptoms (Stevens et al., 1997; Keiler et al., 2013). The therapeutic effects of these phytochemicals are mediated by their estrogen-like activity due to their structural similarity to endogenous estrogens, but they could also cause endocrine disruption with chronic dietary exposure (Kang et al., 2021). Currently, it remains unclear which physiological levels of these compounds potentially cause endocrine disruption and it is crucial to understand the exposure doses needed to achieve these levels.

The most abundant polyphenol in the hop flower itself is xanthohumol (XN); it is marketed in supplement form for its supposed anti-oxidant, anti-inflammatory, and *in vitro* anti-tumor properties considered to arise from its activity in modulating tumor-promoting cell signaling (Vesaghhamedani et al., 2022). However, these hop polyphenols are biochemically interconvertible, and their composition depends on the product preparation process (Bolton et al., 2019). During beer brewing, thermal processing converts XN into isoxanthohumol (iXN), which is a weak ER agonist (Overk et al., 2005). Additionally, the remaining XN is partially converted to iXN in the stomach through acid-catalyzed cyclization (Nikolic et al., 2005). While iXN is only a weakly potent estrogen receptor agonist, it can be metabolically activated by hepatic CYP1A2 (Guo et al., 2006) or the gut microbiota (Possemiers et al., 2005) to the potent phytoestrogen 8-prenylnaringenin (8-PN), in addition to lesser extents of the latter being also present in hops (Fig. 1). The amount of 8-PN present in beer varies widely, ranging from 1 μg/L reported in European lager beer and up to 240 μg/L in American porter beer (Stevens and Page, 2004).

8-PN is the most potent phytoestrogen known to date, with its affinity to ERs being an estimated 100 times higher than the soy isoflavone genistein and only seventy times lower than the endogenous 17 β-estradiol (Schaefer et al., 2003). 8-PN has a more than 2-fold higher affinity for ERα than for ERβ (Schaefer et al., 2003). Moreover, the C8-prenyl group of 8-PN interacts with the lipophilic regions of the ERα binding pocket, which enhances the binding affinity (Mbachu et al., 2020). The two receptors have different effects on cell signaling in various tissues, for example, ERα

---

* Corresponding author. Laboratory of Toxicology, ETH Zürich Schmelzbergstrasse 9, LFO D15.2, Zürich, 8092, Switzerland.
  E-mail address: georg.aichinger@hest.ethz.ch (G. Aichinger).

activation is associated with cell proliferation and ERβ activation is associated with counteracting ERα-stimulated cell proliferation (Rietjens et al., 2013). ERα is the predominant isoform in the uterus, and it is highly expressed in the endometrium, ovaries, mammary gland, and bones. Therefore, ERα activation by 8-PN may affect the regulation of metabolism and endocrine processes (Mauvais-Jarvis et al., 2013).

Given the endocrine activity of 8-PN, there is a concern about its potential endocrine-disrupting properties. So far, research has primarily focused on its beneficial effects as an antioxidant and potential natural hormone replacement, with limited studies addressing its potential adverse impacts, as recently reviewed (Pohjanvirta and Nasri, 2022). For example, Overk et al. (2008) evaluated the estrogenic effects of 8-PN in an adult rat model assessing its impact on uterus weight, demonstrating a clear dose-response relationship. Specifically, the middle and the highest doses of 8-PN in the study, (4 and 40 mg/kg/d) exhibited significant estrogenic activity, resulting in increased uterine weight. Although the estrogenic activity of 8-PN has been demonstrated, a gap in knowledge remains regarding its effects in human target tissues including when 8-PN is combined with other hop polyphenols and endogenous estrogens.

Accurately predicting *in vivo* outcomes from *in vitro* methods remains a challenge, in part due to the compounds' complex toxicokinetic parameters (absorption, distribution, metabolism, and excretion; ADME), which play a crucial role in determining target organs of potential toxicity and the time to reach an internal concentration of the compounds of interest, sensitive exposure windows, species, and sex differences (Svingen et al., 2022). There are several available *in vitro* methods to test endocrine activity (Baker, 2001), however, concentrations of chemicals tested *in vitro* often do not correspond with concentrations at the target sites *in vivo*, raising questions about the relevance of the results to realistic exposure scenarios.

Understanding the toxicokinetics of iXN and 8-PN is essential for predicting their systemic and tissue concentrations and estimating the concentration at target sites where toxicity would occur. Therefore, the aim of this study was to enable prediction of systemic and tissue concentrations of iXN and 8-PN upon ingestion of hops supplements containing both iXN and 8-PN by developing a corresponding physiologically based kinetic (PBK) model that uses human physiology, physicochemical properties, and *in vitro* metabolism data. We established a PBK model specifically parameterized to reflect female physiology, which is physiologically relevant for these exposures. The new model facilitates the estimation of blood and tissue concentrations of iXN and 8-PN, particularly in the context of high ER expression, providing insight into their safety and potential endocrine activity.

2. Methods

2.1. Chemicals and reagents

Pooled Human Liver S9 (mixed gender and age donors), isoxanthohumol (primary reference standard, purity ≥90.0%), 8-prenylnaringenin (analytical standard, ≥95.0%), uridine-5′-diphosphoglucuronic acid (UDPGA) trisodium salt, magnesium dichloride, β-glucuronidases (from bovine liver, 100000 units), and sodium acetate were purchased from Sigma-Aldrich (Buchs, Switzerland). Pooled human intestinal S9 fraction (19 donors, mixed gender) was purchased from Biopredic (Saint-Grégoire, France). Alamethicin was purchased from Enzo Life Sciences AG (Lausen, Switzerland). DMSO was purchased from VWR (Dietikon, Switzerland), and acetonitrile (HPLC-grade) was purchased from Merck-Millipore (Schaffhausen, Switzerland). Dulbecco's Modified Eagle Medium, fetal bovine serum, HBSS, HEPES, and penicillin/streptomycin were purchased from Gibco, Life Technologies Limited (Paisley, UK) and Transwell® inserts were purchased from Corning Incorporated (Kennebunk, USA).

2.2. Glucuronidation kinetics

To quantify hepatic phase II metabolism of iXN and 8-PN, the glucuronidation rates catalyzed by pooled human liver and intestinal S9 fractions of mixed age and gender donors were measured. The incubation mixtures had a final volume of 160 μL and contained 10 mM UDPGA in 50 mM Tris-HCl pH 7.4, 10 mM MgCl$_2$, 0.1 mg/mL hepatic or 0.3 mg/mL intestinal S9 fraction in 0.1 M Tris HCl pH 7.4. The incubation mixtures were pre-incubated without the substrate for 5 min at 37 °C with a final concentration of 25 μg/mL alamethicin to increase membrane porosity. To initiate the reaction, the substrates were added at 100 times the concentration in DMSO. All mixtures were incubated for 15 min at 37 °C except the intestinal S9 8-PN mixtures, which were incubated for 5 min. Rate constants for the glucuronidation reaction were determined using final substrate concentrations ranging from 0.25 to 100 μM. To terminate the reaction 1:1 ratio of ice-cold methanol was added to the samples. Due to the unavailability of reference glucuronides, additional peaks observed in the HPLC analysis after S9 incubations were confirmed to result from glucuronidation by adding 50 μL of the samples to 0.1 M sodium acetate (pH 5) that contained 1000 units of β-glucuronidase. These mixtures were incubated for an additional 1 h at 37 °C and terminated by the addition of the corresponding volume of ice-cold methanol. Samples were kept at −20 °C for 1 h to allow proteins to precipitate. Before analysis, the S9 samples were centrifuged at 20' 817 g for 5 min at 4 °C. The resulting samples were analyzed by HPLC, as described in section 2.2. Curve fitting of the data to Michaelis-Menten kinetics and the calculation of kinetic parameters were conducted using GraphPad Prism 10 software. The glucuronidation rates were scaled to the human organism based on the mg of S9 protein
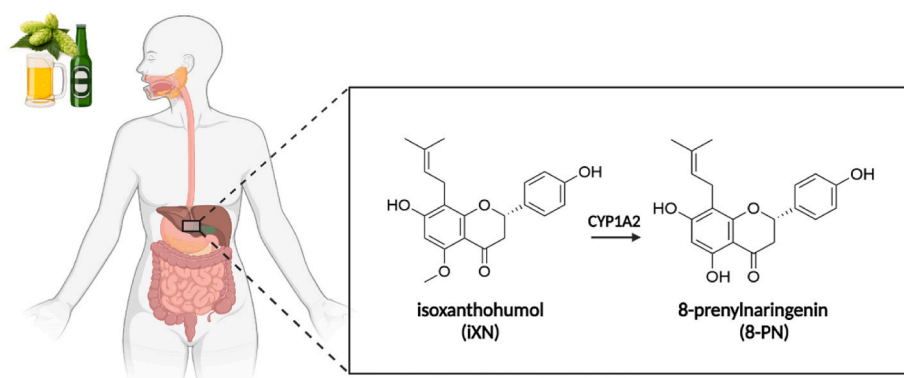

Fig. 1. Schematic representation of biotransformation of isoxanthohumol to 8-prenylnaringenin, including their respective chemical structures.

to g of liver and small intestine with scaling factors commonly used for PBK modeling (VLS9 = 107.3 mg S9 protein/g liver: Wang et al., 2020); (VGS9 = 35.2 mg S9/g small intestine: Peters et al., 2016).

2.3. HPLC analysis

Original compounds and their corresponding glucuronides were quantified using HPLC-DAD analysis on an Agilent 1200 (Agilent Technologies, Santa Clara, California, USA) series instrument. The HPLC system was equipped with a Waters XBridge BEH 130 C18 column, 3.5 μm particle size, 4.6 × 150 mm, and a DAD detector (Agilent Technologies, Santa Clara, California, USA) detecting at 295 nm. The liquid phase consisted of water (A) and acetonitrile (B), each supplemented with 0.1% formic acid. The following gradient profile was used at a flow rate of 1 mL/min: 0 min, 20% B; 0–2 min, 50% B; 10–14 min, 80% B; 14–15.5 min, 20% B; post-time 3 min. Reference standards of iXN and 8-PN were used to generate corresponding calibration curves for quantification.

2.4. PBK model conceptualization

The PBK model for hop polyphenols developed in this study was based on a previously published model for urolithin A and its glucuronide (Aichinger et al., 2023), which was slightly modified and adapted to include organs of interest for estrogenic activity, such as the uterus. The model consists of blood, adipose, liver, gut, uterus, and kidney tissue as separate compartments (Fig. 2). The implementation of the uterus as a compartment was based on Teeguarden et al. (2005), where the uterus partition coefficient was assumed to be the same as the muscle partition coefficient, as the uterus is primarily composed of muscle tissue. Other organs were grouped as slowly perfused tissues (bone, skin, and muscle) and quickly perfused tissues (heart, brain, and lungs). Uptake of iXN was modeled to occur via the small intestinal lumen, and excretion was modeled to occur via the kidneys. As both iXN and 8-PN undergo

glucuronidation in the liver and small intestinal tissue, the glucuronidation rates were measured as described above and implemented in the model. A separate submodel was created to predict the levels of iXN and 8-PN glucuronide (iXNGluc, 8-PNGluc) and 8-PN. Additionally, the conversion rate of iXN to 8-PN in the liver was modeled as described below. The main model was extended to three submodels, for iXNGluc, 8-PNGluc, and 8-PN.

2.5. Cell culture and Caco-2 permeability assay

The Caco-2 human colon carcinoma cell line was cultured in Dulbecco's Modified Eagle Medium (DMEM) supplemented with 1% (v/v) fetal bovine serum (FBS) and 1% (v/v) penicillin/streptomycin (P/S) for three weeks before seeding into Transwell® 0.4 μm pore polycarbonate membrane 12-well plates. The media was changed every second day for 24 ± 2 days prior to performing permeability assays. The cells were seeded on Transwell® polycarbonate membrane and the permeability assays were performed on day 24 or ± 2 days. The cell culture media was changed 12–24 h prior to performing the permeability assays. Additionally, the transepithelial electrical resistance (TEER) of each monolayer was measured and was well above 300 Ωcm^{-2}, indicating good monolayer integrity. On the day of the permeability assays, the Caco-2 monolayer was washed with HBSS containing 25 mM HEPES (HBSS/HEPES) at pH 7.4 on both apical and basolateral side for 20 min on a shaking incubator (50 rpm, 37 °C). Test solutions of 50 μM iXN and 8-PN in HBSS/HEPES were prepared from stock solutions in DMSO (DMSO concentration was below 0.1%). The test solutions of iXN and 8-PN were added to the apical side of the monolayers and blank HBSS/HEPES to the basal side for measuring the apical to basolateral side permeability. From the basolateral side, samples were collected at selected time points (0, 5, 10, 20, 30, 60, 90, 120 min) and the apical side at time points 0 and 120 min. The amount of sample taken from the basolateral site was always replaced with the same amount of HBSS/HEPES. All samples were analyzed by LC-MS (Thermo Fisher Scientific, Waltham, Massachusetts,
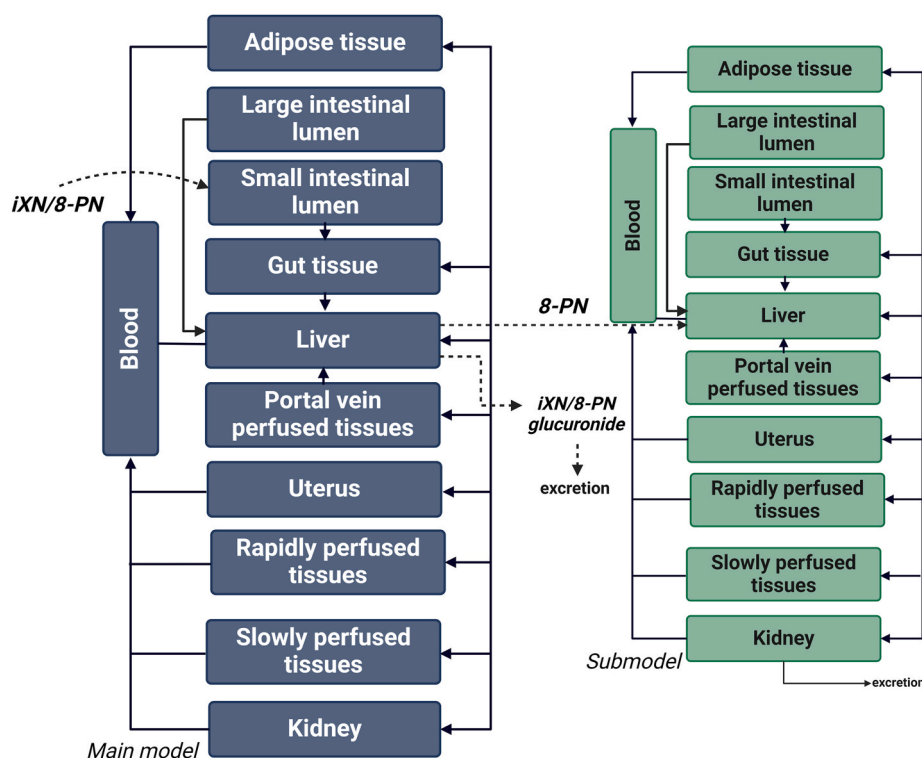

Fig. 2. The structural concept of the PBK model, with the main model (blue) for iXN and the submodel (green) for 8-PN. The submodels for iXN and 8-PN glucuronides are not shown in the model. The dashed lines indicate transferring processes between the two submodels, uptake or excretion. (For interpretation of the references to color in this figure legend, the reader is referred to the Web version of this article.)

USA). Afterwards, the Caco-2 cell monolayer was washed three times with ice-cold PBS, the cells were detached by scraping, and ice-cold methanol was added to collect them for LC-MS analysis. Four independent experiments were performed, each comprised of four technical replicates.

2.6. Model parametrization

The PBK model was parameterized using a standard average female body weight of 60 kg. Relative tissue volumes and blood flow rates to the respective organs reported for women (Valentin), small and large intestinal lumen volumes (Mendez-Catala et al., 2021), and gastrointestinal transit times (Wang et al., 2015) were incorporated. The relative tissue volume and blood flow rates for the portal vein-perfused tissues were calculated as a single value. Gastrointestinal anatomical parameters were calculated as previously described (Mendez-Catala et al., 2021). The glomerular filtration rate was obtained from the literature and set to 125 mL/min/(173 m^2) (Levey et al., 2014). Compound-specific physiochemical parameters were calculated from LogP and pK$_a$ values for iXN (LogP 4.1, pK$_a$ 7.6 ; Moens et al., 2020), 8-PN (LogP 4.3, pK$_a$ 7.7; Moens et al., 2020) and their glucuronides (iXNGluc, LogP 1.61, pK$_a$ 8.55; 8-PNGluc LogP 1.34, pK$_a$ 7.87 obtained from ChemDraw 19.0 Software) by using the QIVIVE toolbox (Punt et al., 2021). The toolbox calculates the tissue partition coefficient on the Rodges and Rowland method and the fraction unbound in plasma (fup) on Lobell and Sivarajah (Rodgers and Rowland, 2006; Lobell, 2003). The K$_m$ (17.17 μM) and V$_{max}$ (5.47 pmol/min/pmol) for the conversion of iXN to 8-PN in the liver were reported in the literature, measured in human liver microsomes by CYP1A2 (Guo et al., 2006). The CYP1A2 conversion of iXN to 8-PN was scaled based on the intersystem extrapolation factor for CYP1A2 (ISEF), the P450 abundance pmol/mg protein, and the amount of microsomes/liver weight (Chen et al., 2011). The absorption of iXN and 8-PN was predicted based on the apparent permeability coefficient (P$_{app}$) measured *in vitro* and scaled to an *in vivo* P$_{app}$ as described below. All parameters used can be found in the PBK model code in the supporting information. The input dose was based on a human intervention study in which postmenopausal women took three doses of a hops supplement (van Breemen et al., 2014). The data measured in the study was used to evaluate the accuracy of the PBK model predictions.

2.7. Sensitivity analysis

A sensitivity analysis was performed to evaluate the effect of parameter variation on the model predictions. To perform the sensitivity analysis, each parameter was increased by 5%, and the model was run at the dose given in the human intervention study. Using the formula developed by Evans and Andersen (2000):

$$SC = (C' - C) / (P' - P) \times P / C$$

The normalized sensitivity coefficients (SC) were calculated, with C and C′ referring to the peak concentration of iXN in blood with unchanged or increased parameters, respectively, P and P' referring to the value of the unchanged or increased parameter of interest.

2.8. Predictions of iXN and 8-PN concentrations in tissues of interest

The PBK model was used to predict systemic and tissue concentrations of both iXN and 8-PN in all tissue compartments, including the uterus, which is considered of high relevance. The intake was based on different dosing scenarios administered *in vivo* in the study by van Breemen et al. (2014a).

2.9. LC-MS analysis of permeability assays and calculation of absorption kinetics

Samples from the Caco-2 permeability studies were centrifuged at 20' 817 g for 15 min at 4 °C prior to LC-MS analysis. All samples were analyzed using a Vanquish HPLC coupled to an IDX tribrid mass spectrometer. The chromatographic separation of analytes was achieved using a Phenomenex Synergi™ 4 μm Polar-RP (80 Å, 30 × 2 mm) column. The column compartment was set to 40 °C and the samples were stored in the autosampler cooled to 4 °C. The injection volume was 5 μL. The mobile phases were water (solvent A), and acetonitrile (solvent B) LC-MS grade, each supplemented with 0.1% formic acid. The flow rate was 0.7 mL/min, and the gradient was as follows: 0 min (5% B), 0.1 min (5% B), 1.8 min (100% B), 2.4 min (5% B), and 2.7 min (5% B). To protect the MS from HBSS, for the first 1.25 and last 0.6 min, the divert valve was set to waste. The MS parameters were negative ion spray voltage at 2500 V, sheath gas, auxiliary gas, and sweep gas at 60, 15, and 2 Arb, respectively, and ion transfer tube and vaporizer temperature at 350 and 400 °C, respectively. The P$_{app}$ was calculated using the following formula (Hubatsch et al., 2007):

$$P_{app} = \frac{dQ}{dt} * \frac{1}{(A*C0)}$$

In the formula, dQ/dt is the steady-state flux (μM/s), change of concentration over time, A is the surface area of the Transwell®, and C0 is the initial concentration (μM) in the apical side. The mean P$_{app}$ values for iXN and 8-PN derived from four independent experiments were scaled to *in vivo* P$_{eff}$ (effective permeability) values using the algorithm of Sun et al. (2002). These values were implemented in the PBK model in order to predict the absorption of both iXN and 8-PN absorption.

3. Results

3.1. In vitro glucuronide conjugation of iXN and 8-PN

Kinetic parameters for liver and intestinal phase II rates of glucuronidation of iXN and 8-PN were determined by incubation with human pooled hepatic and intestinal S9 fractions. For both iXN and 8-PN, the formation of glucuronides was observed as the appearance of one peak that was observed only when incubations were performed in the presence of UDPGA. No peaks corresponding to glucuronides were observed in the respective control without UDPGA. The glucuronide formation followed Michaelis-Menten kinetics, resulting in affinity constants (K$_m$) of 6.33 μM for hepatic and 6.06 μM for intestinal S9 fraction for iXN. The V$_{max}$ values for iXN were equal to 1.6 and 0.79 nmol/mg/min for hepatic and intestinal S9 fractions, respectively (Fig. 3). The K$_m$ values of 8-PN were 0.79 μM and 0.32 μM and V$_{max}$ 0.76 and 1.250 nmol/mg/min for hepatic and intestinal S9, respectively. These results suggest that the glucuronidation of both iXN and 8-PN occurs rapidly in both, hepatic and intestinal tissues.

3.2. Caco-2 cell permeability assay

To estimate the gastrointestinal permeability of iXN and 8-PN, Caco-2 (human colorectal adenocarcinoma) cells were cultured to form a monolayer in a Transwell® polycarbonate membrane system. The transfer of the compounds from the apical to the basolateral side was measured. Concentrations of both substances increased linearly in the basolateral compartment over at least 90 min. The P$_{app}$ was calculated to be $6.06 \pm 2.98 \times 10^{-6}$ cm/s for iXN, and $7.22 \pm 1.66 \times 10^{-6}$ cm/s for 8-PN, respectively. These values indicate moderate permeability for both compounds, with 8-PN transferring slightly faster than iXN.
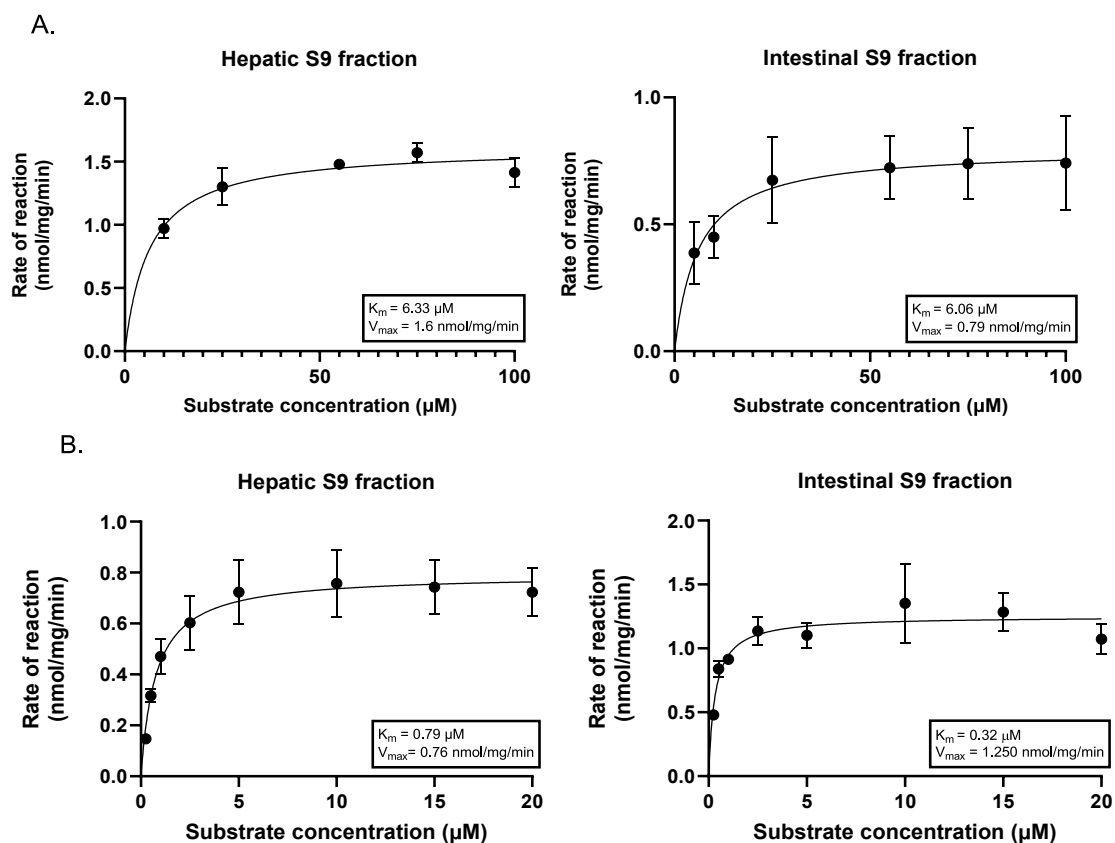
A.

B.

Fig. 3. *In vitro* glucuronidation rates of iXN (A) and 8-PN (B) by hepatic and small intestinal S9 fractions. The iXN/8-PN-concentration-dependent formation rates are shown. Data are shown as mean ± SD of three experiments. The lines represent curve fits to the Michaelis-Menten equation.

3.3. Comparison of the PBK model predictions with in vivo data from a human intervention study

The fully parameterized PBK model was run using starting doses of 0.8 mg, 1.6 mg, and 3.2 mg iXN, matching the conditions of a human intervention study (van Breemen et al., 2014a). Serum concentrations (C_{max} values) of total iXN (iXN + iXNGluc) were predicted and compared to the previously published *in vivo* results (Fig. 4A). These values matched well, supporting the accuracy of the model. The time required to reach the C_{max} (T_{max}) predicted by the model was 7 h 47 min for the lowest and mid-dose and 7 h 45 min for the highest administered

dose. In the dietary intervention study, the reported time required to reach the maximal concentration in blood ranged from 1.8 h up to 7.5 h across the different doses, indicating a large deviation amongst the subjects (van Breemen et al., 2014a).

Considering the large variation detected in the samples of the selected human intervention study, the model's predictions were considered sufficiently accurate, and the small deviation in T_{max} values as compared to reported average values was considered acceptable. Additionally, the simulated C_{max} values for 8-PN glucuronide were compared to measured 8-PN blood concentrations (Fig. 4B). These closely matched all three *in vivo* doses. Taking all comparisons of
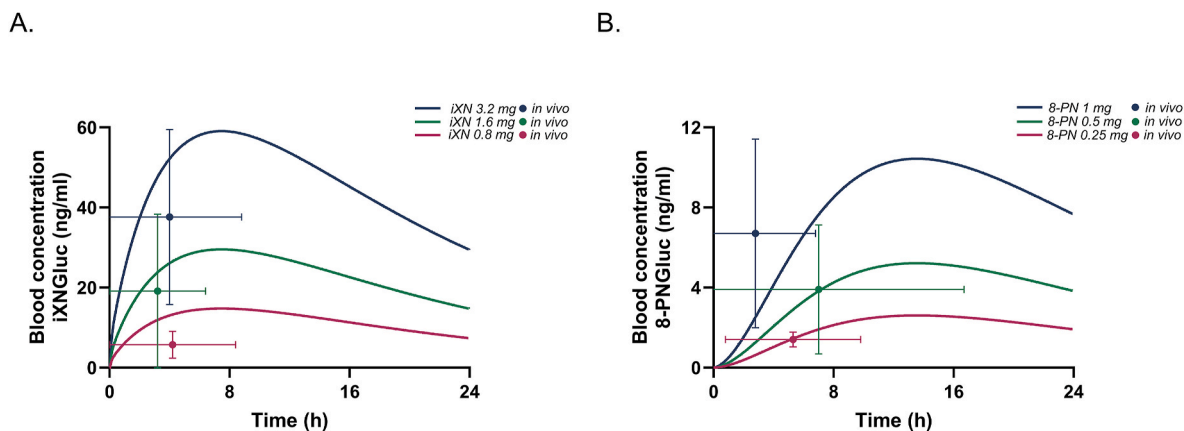
A.

B.

Fig. 4. Curves representing predicted blood concentrations of iXN glucuronide (A) and 8-PN glucuronide (B) after supplementation with three doses of iXN and 8-PN from a hop supplement, compared with previously reported blood C_{max} and T_{max} values by van Breemen et al., (2014a). Curves represent PBK model–simulated blood concentrations over time, while circles represent the mean ± SD of C_{max} and T_{max} reported in the human intervention study.

predicted to measured C_{max} values into consideration, the model provided adequate accuracy in predicting time-dependent blood concentrations of iXN and 8-PN glucuronides.

3.4. Sensitivity analysis

A sensitivity analysis was performed to assess which physiological parameters highly influence predicted blood concentrations of iXN and iXNGluc (Fig. 5A). Exposure to a single dose of 0.8 mg iXN was modeled, corresponding to the lowest used dose by van Breemen et al. (2014a). The predicted blood concentrations of iXN and iXNGluc were predominantly affected by body weight and the $logP_{app}$ value of iXN. Parameters describing hepatic and intestinal metabolism of iXN also affected systematically available concentrations substantially. Specifically, the hepatic metabolism had a considerable impact with a sensitivity coefficient (SC) of -0.92 for V_{max} and 0.97 for K_m. Besides metabolism, gastrointestinal parameters, including passing time through the small

intestine and the area of small and large intestines, had SCs of -0.44, -0.16, and 0.57, respectively. Additionally, iXNGluc levels were slightly affected by the parameters describing glomerular filtration rate (GFR), slowly perfused tissue/blood partition coefficient (PSIXNGluc), fat/-blood partition coefficient (PFIXNGluc), and faction unbound in plasma (FUIXNGluc). To a lesser extent, iXNGluc concentrations were influenced by gastrointestinal physiological parameters, including the volume and area of the small and large intestines. The predictions were also affected by the physiological parameter for the relative volume of adipose tissue. Regarding 8-PN, the sensitivity analysis was performed the same way as for iXN using exposure to a single dose of 0.25 mg 8-PN corresponding to the lowest dose by van Breemen et al. (2014a) (Fig. 5B). The predicted blood concentrations of 8-PN and 8-PNGluc were affected predominantly by the same parameters as for iXN and iXNGluc including the $logP_{app}$ value of 8-PN being the most influential parameter.
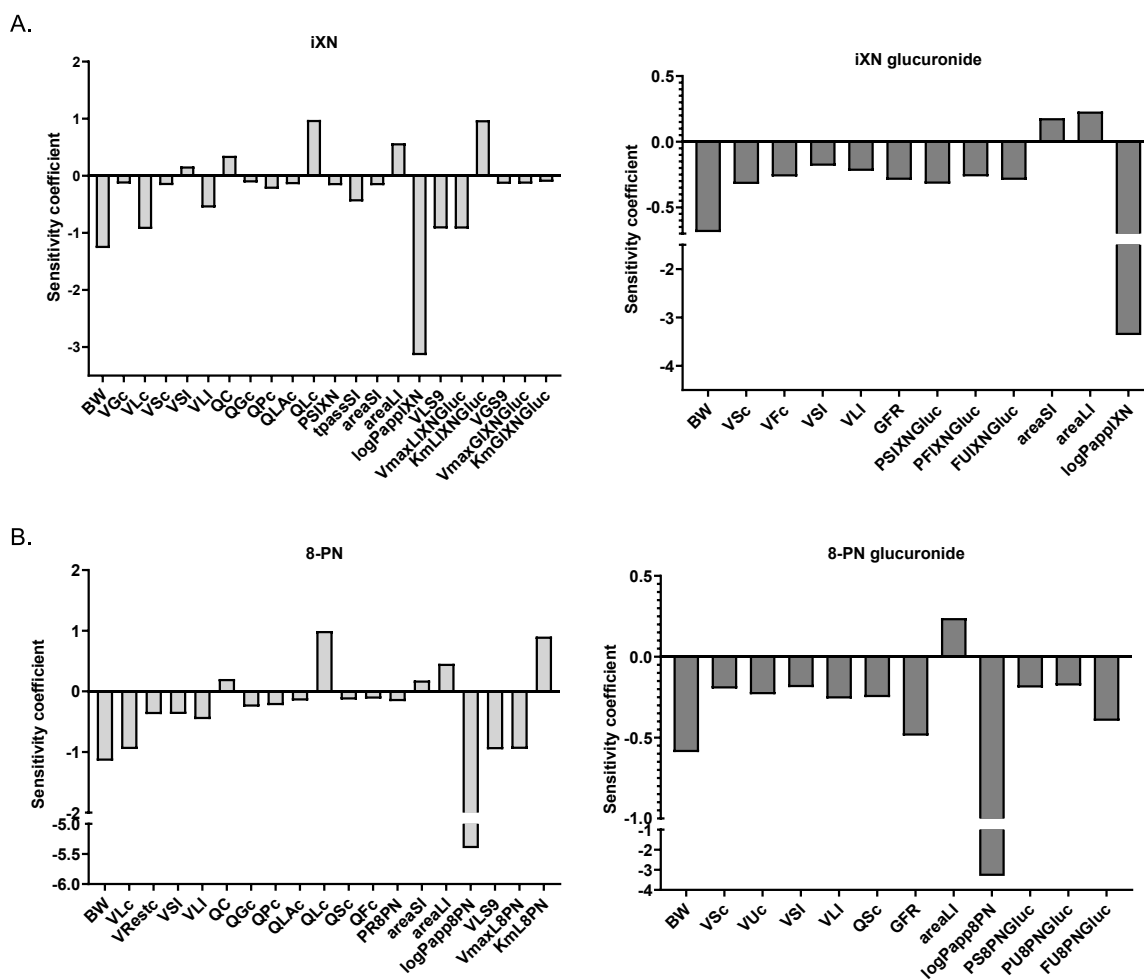

Fig. 5. Sensitivity of model parameters (A. iXN and iXNGluc, B. 8-PN and 8-PNGluc), displayed as normalized sensitivity coefficients (SC) that were calculated from the alteration of blood C_{max} values caused by a 5% elevation of the respective parameter. Parameters with an absolute SC > 0.1 are shown and abbreviated as: BW, bodyweight; VGc, relative gut tissue (small intestine) volume; VLc, relative liver tissue volume; VSc, relative slowly perfused tissues volume; VFc, relative adipose tissue volume; VUc, relative tissue volume of the uterus; Vrestc, relative tissue volumes of all tissue not included in the model; VSI, volume of the small intestinal lumen; VLI, volume of the large intestinal lumen; QC, cardiac output; QGc, fraction of blood flow to gut; QPc fraction of blood flow to portal vein perfused tissues; QLA, fraction of blood flow to liver via artery; PSIXN/PSIXNGluc/PS8PNGluc, slowly perfused tissue/blood partition coefficient; tpassSI, passing time through the small intestine; areaSI, surface area of the small intestinal lumen; areaLI surface area of large intestinal lumen; logPappIXN, logarithm of the permeability coefficient across the intestinal barrierof iXN; logPapp8PN, logarithm of the permeability coefficient across the intestinal barrier of 8-PN; VLS9, scaling factor for S9 protein to liver tissue; VmaxLIXNGluc, maximal velocity of hepatic glucuronidation of iXN, KmLIXNGluc, affinity constant for hepatic iXN glucuronidation; VGS9, scaling factor for S9 protein to intestinal tissue; VmaxGIXNGluc, maximal velocity of intestinal glucuronidation of iXN, KmGIXNGluc, affinity constant for intestinal iXN glucuronidation; GFR, glomerular filtration rate; PFIXNGluc, fat/blood partition coefficient; FUIXNGluc, FU8PNGluc faction unbound of iXNGluc and 8-PNGluc; PR8PN, rapidly perfused tissue/blood partition coefficient; QSc, fraction of blood flow to slowly perfused tissues; QFc, fraction of blood flow to fat; VmaxL8PN, maximal velocity of hepatic 8-PN glucuronidation; KmL8PN, affinity constant for hepatic 8-PN glucuronidation.

3.5. Predictions of iXN and 8-PN concentrations in blood and tissues of interest

Following the model evaluation, the model was used to simulate the systemic concentrations of iXN and 8-PN in their aglyconic bioactive form, based on three different dosing scenarios described in a human intervention study (van Breemen et al., 2014a). Besides the single dose, a repeated dose scenario of taking the hops supplement for 5 days was also tested. Following the highest dose (3.6 mg of iXN and 1 mg of 8-PN daily), the maximal blood levels of iXN and 8-PN were predicted to be 0.13 nM and 0.008 nM, respectively (Fig. 6). Additionally, following the same scenario, tissue levels of iXN and 8-PN were predicted to be in the low picomolar range for all selected organs of interest (i.e. liver, kidneys, uterus, adipose tissue; Fig. 7). Of note, both for iXN and 8-PN our model predicts the substances to be slightly accumulated in adipose tissue after 24 h.

Further, the model was used to predict blood and uterus concentrations of iXN and 8-PN following a dosing scenario of 1 beer daily for 7 days (Table 1). The specific amounts of iXN and 8-PN in beers used as an input dose for the PBK model were obtained from Stevens and Deinzer (1999) are shown in Table 2.

4. Discussion

In this study, a PBK model was developed to estimate systemic concentrations of the estrogenic hop polyphenols isoxanthohumol and 8-prenylnaringenin, and their metabolites in women. The model integrates hepatic and intestinal glucuronidation kinetics measured using S9 fractions, human physiological parameters derived from the literature, tissue partitioning, and plasma binding estimated using quantitative structure-activity relationship (QSAR) tools. Initially, parameters for gastrointestinal permeability were taken from literature, but after sensitivity analysis indicated that the P_{app} of iXN and 8-PN was the most influential parameter for the prediction of C_{max}, we decided to confirm these values experimentally. Therefore, in vitro measurements of intestinal permeability of iXN and 8-PN were conducted using a Caco-2 cell monolayer Transwell® system. P_{app} coefficients for iXN and 8-PN indicated a moderate permeability for both compounds, with values between those reported in the literature (EMA, 2014; Nikolic et al., 2006). Variability of Caco-2 data, often observed across different laboratories, is attributed to factors including the passage number of the Caco-2 cells, pH conditions, and the integrity of the monolayer (Press, 2008).

To evaluate the accuracy of the model's predictions, the predicted blood concentrations of iXNGluc and 8-PNGluc were compared to the respective blood concentrations reported from a human intervention study (van Breemen et al., 2014b). This comparison revealed only a 1.5-fold difference between predicted and in vivo measured levels of total (conjugated plus aglycone) iXN blood levels, whereas the predicted levels of 8-PN were even more closely aligned with those measured in the in vivo study (Fig. 4). A limitation in evaluating the model was the limited availability of suitable human intervention studies. Research studies have primarily focused on xanthohumol, the precursor of iXN, administered as a single compound in rats (Legette et al., 2012) and humans (Legette et al., 2014) to monitor the in vivo formation of iXN and 8-PN. We identified three studies that administered iXN (van Breemen et al., 2014a, 2020; Bolca et al., 2010), but also administered the compound in mixtures with co-occurring polyphenols, including 8-PN, at different doses. Therefore, the blood levels of 8-PN could result from both, the initial dose of 8-PN and/or its conversion from iXN. From the published human intervention studies, the study by van Breemen et al. (van Breemen et al., 2014a) was selected for model evaluation because of its detailed reporting of hop polyphenol content in the supplements and pharmacokinetic parameters, including C_{max} and T_{max} for both iXN and 8-PN. In their study, postmenopausal women were taking a hop supplement containing XN, iXN, 8-PN, and 6-prenylnaringenin either at low, medium, or high doses for 5 days. The applicability of their study to evaluate PBK models is limited by the small sample size (5 subjects), a treatment period of 5 days per dose, and the absence of additional information, e.g. reporting of individual values or subject physiology (BW, BMI). The study reported two peak concentrations of iXN and 8-PN in blood, indicating the occurrence of enterohepatic recirculation. Future models of hop polyphenols could consider incorporating enterohepatic circulation.

The PBK model was parameterized to incorporate the hepatic conversion of iXN to 8-PN by the human liver enzyme CYP1A2, based on in vitro studies with CYP1A2 and human microsomes (Guo et al., 2006). CYP1A2 activity is influenced by genetic polymorphisms and environmental exposures that act as inducers (e.g., cigarette smoking) or inhibitors (e.g., oral contraceptives)(Koonrungsesomboon et al., 2018). These factors could impact systemic levels of 8-PN after iXN exposure, suggesting variable metabolic conversion among individuals. For future studies, it could be interesting to further extend the PBK model to account for genetic polymorphisms of CYP1A2, which would potentially predict the systemic concentrations of target compounds for each CYP1A2 genotype group.

Based on realistic dosing scenarios, the PBK model provides initial insights into tissue concentrations of both iXN and 8-PN, suggesting maximal concentrations in the low picomolar range. In a recent study, a detailed assessment of 8-PN was performed by comparing various in vitro and in vivo methods standardized by the organisation for economic cooperation and development (OECD) (Sim et al., 2022). The results of the study showed point of departure (POD) for 8-PN at 0.29 μM and 0.029 μM for ERα dimerization and ER transactivation. Additionally, it was shown that 8-PN exhibits significant estrogenic activity, with PC50
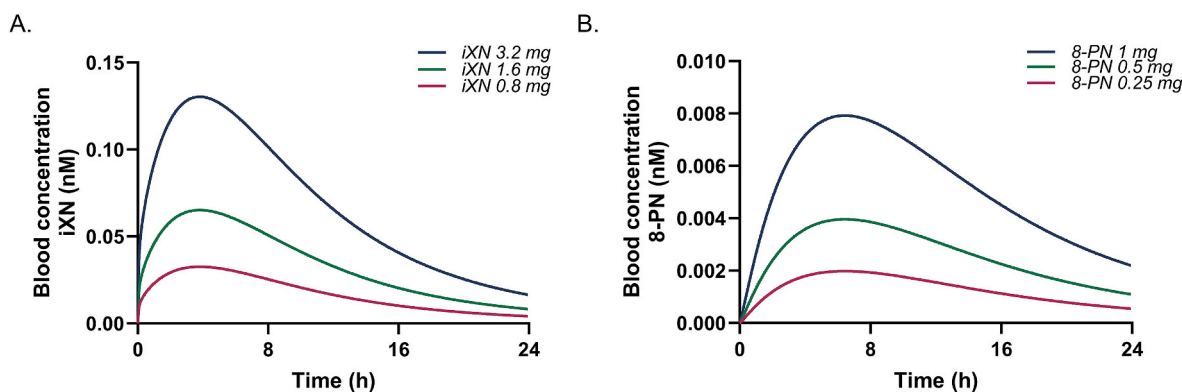

Fig. 6. Blood concentrations of iXN (A) and 8-PN (B) following three different dosing scenarios after supplementation with a hop supplement, as predicted by the PBK model. Blue lines represent the highest dose, green middle dose and pink represents the lowest administered dose. (For interpretation of the references to color in this figure legend, the reader is referred to the Web version of this article.)
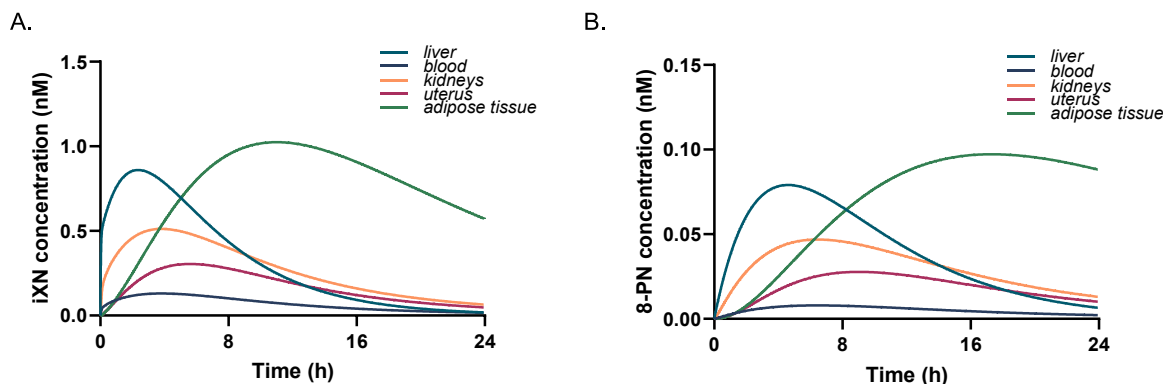
Fig. 7. Predicted levels of iXN (A) and 8-PN (B) in organs of interest after supplementation with the highest dose of a hop supplement (3.2 mg of iXN and 1 mg of 8-PN).

Table 1

Blood and uterus C_{max} of iXN and 8-PN after one beer a day for seven days scenario of highly and low-hopped beers.

Highly hopped beers	C_{max} blood iXN (pM)	C_{max} blood 8-PN (pM)	C_{max} uterus iXN (pM)	C_{max} uterus 8-PN (pM)
American porter	59.32	2.32	139.13	8.19
Strong ale	153.20	1.11	360.10	3.94
Low hopped beers				
European lager	1.77	0.01	4.16	0.04
European pilsner	25.43	0.21	59.63	0.74
Alcohol-free beer	4.90	0.03	11.49	0.11

Table 2

Isoxanthohumol and 8-prenylnaringenin levels in beer measured by LC-MS/MS as reported by Stevens and Deinzer, (1999).

Highly hopped beers	Isoxanthohumol (µM)	8-prenylnaringenin (µM)
American porter	3.75	0.705
Strong ale	9.706	0.323
Low hopped beers		
European lager	0.112	0.0029
European pilsner	1.608	0.061
Alcohol-free beer	0.31	0.0088

values (corresponding to the dose required to cause 50% of the system's maximal effect) of 2.14 µM for ER-α dimerization and 139 nM for ER transactivation (Sim et al., 2022). The ER-α dimerization for all compounds tested in the study was less sensitive compared to the ER transactivation. Moreover, a significant increase in uterine weight was observed in an *in vivo* uterotrophic assay, highlighting the estrogenic potential of 8-PN.

Even though this PBK model predicts significantly lower systemic concentrations at the used doses, higher 8-PN levels might be achieved via repeated exposure to hop supplements or hopped beverages. The PBK model was used to test 5 days of repeated exposure to the hop supplement used for the evaluation of the study and the results only shower a minor increase in systemic 8-PN levels. Additionally, the model was also used to predict blood and uterus concentrations of 8-PN and iXN based on highly and low-hopped beer containing both iXN and 8-PN, simulating a scenario of one beer per day for seven days. The model predicted concentrations below 0.1 nM for both high and low-hopped beer scenarios. The internal levels are lower than after hops supplementation.

In an *in vitro* study using Ishikawa cells, slight synergistic estrogenic effects of iXN and 8-PN were demonstrated, indicating an enhancement of estrogenic activity upon the combination of these compounds (Aichinger et al., 2021). This interaction suggests that even at low concentrations, iXN and 8-PN could potentially influence ER-mediated responses, highlighting the need for a thorough further evaluation. Additionally, the presence of endogenous estrogens *in vivo* adds another layer of complexity to their safety testing, as these hormones could potentially interact with the compounds being studied. It is crucial to recognize that the current model includes hepatic and intestinal tissue metabolism and, therefore, does not consider the potential conversion of iXN to 8-PN that was previously demonstrated to be catalyzed by the human gut microbiome. The respective O-demethylation was reported for specific bacteria occurring in the human gastrointestinal tract, e.g. for *Eubacterium limosum* and *E. ramulus* (Possemiers et al., 2005; Paraiso et al., 2019). Additionally, a dietary intervention study of fifty healthy postmenopausal women who consumed a hop supplement showed the ability of the fecal microbiome to convert iXN to 8-PN with varying efficiency, resulting in a classification of poor, moderate, and strong 8-PN producers (Bolca et al., 2007). This variability underscores the potential importance of microbial conversion and the pronounced interindividual differences in metabolism. The incorporation of gut microbial iXN to 8-PN conversion as a separate metabolic compartment in the PBK model could be a valuable approach to differentiate between different metabolizing groups and is envisioned for a follow-up study.

5. Conclusion

The PBK model estimates the systemic and tissue concentrations of hop-derived iXN and 8-PN upon different dosing scenarios. Both iXN and 8-PN blood levels were estimated at low picomolar ranges upon different dosing scenarios. Additionally, the estimated tissue levels of both compounds were also in the low picomolar levels. The model serves as a tool for future quantitative *in vitro* to *in vivo* extrapolation (QIVIVE) to assess endocrine effects occurring *in vivo*.

CRediT authorship contribution statement

Maja Stevanoska: Writing – review & editing, Writing – original draft, Visualization, Methodology, Investigation, Conceptualization. **Karsten Beekmann:** Writing – review & editing, Supervision, Methodology. **Ans Punt:** Supervision, Methodology. **Shana J. Sturla:** Writing – review & editing, Supervision. **Georg Aichinger:** Writing – review & editing, Supervision, Methodology, Conceptualization.

Declaration of Generative AI and AI-assisted technologies in the writing process

During the preparation of this work the authors used DeepL, Grammarly and ChatGPT 4 in order to refine and detect grammar and spelling errors. After using these tools, the authors reviewed and edited the content as needed and take full responsibility for the content of the publication.

Declaration of competing interest

The authors declare that they have no known competing financial interests or personal relationships that could have appeared to influence the work reported in this paper.

Appendix A. Supplementary data

Supplementary data to this article can be found online at https://doi.org/10.1016/j.fct.2025.115247.

Data availability

Data will be made available on request.

References

Aichinger, G., Bliem, G., Marko, D., 2021. Systemically achievable doses of beer flavonoids induce estrogenicity in human endometrial cells and cause synergistic effects with selected pesticides. Front. Nutr. 8, 691872.

Aichinger, G., Stevanoska, M., Beekmann, K., Sturla, S.J., 2023. Physiologically-based pharmacokinetic modeling of the postbiotic supplement urolithin A predicts its bioavailability is orders of magnitudes lower than concentrations that induce toxicity, but also neuroprotective effects. Mol. Nutr. Food Res., 2300009

Baker, V.A., 2001. Endocrine disrupters testing strategies to assess human hazard Toxicol in vitro, 1 (15).

Beral, V., Banks, E., Reeves, G., Bull, D., 2003. Breast cancer and hormone-replacement therapy: the million women Study. Lancet 362 (9392), 1330–1331.

Bolca, S., Possemiers, S., Maervoet, V., Huybrechts, I., Heyerick, A., Vervarcke, S., et al., 2007. Microbial and dietary factors associated with the 8-prenylnaringenin producer phenotype: a dietary intervention trial with fifty healthy post-menopausal Caucasian women. Br. J. Nutr. 98 (5), 950–959.

Bolca, S., Li, J., Nikolic, D., Roche, N., Blondeel, P., Possemiers, S., et al., 2010. Disposition of hop prenylflavonoids in human breast tissue. Mol. Nutr. Food Res. 54 (Suppl. 2), S284–S294 (0 2).

Bolton, J.L., Dunlap, T.L., Hajirahimkhan, A., Mbachu, O., Chen, S.N., Chadwick, L., et al., 2019. The multiple biological targets of hops and bioactive compounds. Chem. Res. Toxicol. 32 (2), 222–233.

Chen, Y., Liu, S., Nguyen, K., Fretland, A.J., 2011. Utility of intersystem extrapolation factors in early reaction phenotyping and the quantitative extrapolation of human liver microsomal intrinsic clearance using recombinant cytochromes P450. Drug Metab. Dispos. 39 (3), 373–382.

EMA, 2014. Assessment Report on *Humulus Lupulus L.*, Flos. HMPC. Report No.: 418902.

Evans, M.V., Andersen, M.E., 2000. Sensitivity analysis of a physiological model for 2,3,7,8-tetrachlorodibenzo-p-dioxin (TCDD) assessing the impact of specific model parameters on sequestration in liver and fat in the rat. Toxicol. Sci. 54, 71–80.

Guo, J., Nikolic, D., Chadwick, L.R., Pauli, G.F., van Breemen, R.B., 2006. Identification of human hepatic cytochrome P450 enzymes involved in the metabolism of 8-prenylnaringenin and isoxanthohumol from hops (Humulus lupulus L.). Drug Metab. Dispos. 34 (7), 1152–1159.

Hubatsch, I., Ragnarsson, E.G., Artursson, P., 2007. Determination of drug permeability and prediction of drug absorption in Caco-2 monolayers. Nat. Protoc. 2 (9), 2111–2119.

Kang, S., Jo, H., Kim, M.R., 2021. Safety assessment of endocrine disruption by menopausal health functional ingredients. Healthcare 9 (10), 1376.

Keiler, A.M., Zierau, O., Kretzschmar, G., 2013. Hop extracts and hop substances in treatment of menopausal complaints. Planta Med. 79 (7), 576–579.

Koonrungsesomboon, N., Khatsri, R., Wongchompoo, P., Teekachunhatean, S., 2018. The impact of genetic polymorphisms on CYP1A2 activity in humans: a systematic review and meta-analysis. Pharmacogenomics J. 18 (6), 760–768.

Legette, L., Ma, L., Reed, R.L., Miranda, C.L., Christensen, J.M., Rodriguez-Proteau, R., et al., 2012. Pharmacokinetics of xanthohumol and metabolites in rats after oral and intravenous administration. Mol. Nutr. Food Res. 56 (3), 466–474.

Legette, L., Karnpracha, C., Reed, R.L., Choi, J., Bobe, G., Christensen, J.M., et al., 2014. Human pharmacokinetics of xanthohumol, an antihyperglycemic flavonoid from hops. Mol. Nutr. Food Res. 58 (2), 248–255.

Levey, A.S., Inker, L.A., Coresh, J., 2014. GFR estimation: from physiology to public health. Am. J. Kidney Dis. 63 (5), 820–834.

Lobell, M.S.V., 2003. In silico prediction of aqueous solubility, human plasma protein binding and volume of distribution of compounds from calculated pK a and AlogP98 values. Mol. Divers. 7, 69–87.

Mauvais-Jarvis, F., Clegg, D.J., Hevener, A.L., 2013. The role of estrogens in control of energy balance and glucose homeostasis. Endocr. Rev. 34 (3), 309–338.

Mbachu, O.C., Howell, C., Simmler, C., Malca Garcia, G.R., Skowron, K.J., Dong, H., et al., 2020. SAR study on estrogen receptor α/β activity of (iso)flavonoids: importance of prenylation, C-Ring (un)saturation, and hydroxyl substituents. J. Agric. Food Chem. 68 (39), 10651–10663.

Mendez-Catala, D.M., Wang, Q.R., Rietjens, I.M.C.M., 2021. PBK model-based prediction of intestinal microbial and host metabolism of zearalenone and consequences for its estrogenicity. Mol. Nutr. Food Res. 65 (23), 2100443.

Moens, E., Bolca, S., Van de Wiele, T., Van Landschoot, A., Goeman, J.L., Possemiers, S., et al., 2020. Exploration of isoxanthohumol bioconversion from spent hops into 8-prenylnaringenin using resting cells of Eubacterium limosum. Amb. Express 10 (1), 79.

Narod, S.A., 2011. Hormone replacement therapy and the risk of breast cancer. Nat. Rev. Clin. Oncol. 8 (11), 669–676.

Nikolic, D., Li, Y.M., Chadwick, L.R., Pauli, G.F., van Breemen, R.B., 2005. Metabolism of xanthohumol and isoxanthohumol, prenylated flavonoids from hops (*Humulus lupulus L.*), by human liver microsomes. J. Mass Spectrom. 40 (3), 289–299.

Nikolic, D., Li, Y., Chadwick, L.R., van Breemen, R.B., 2006. In vitro studies of intestinal permeability and hepatic and intestinal metabolism of 8-prenylnaringenin, a potent phytoestrogen from hops (*Humulus lupulus L.*). Pharm. Res. (N. Y.) 23 (5), 864–872.

Overk, C.R.Y.P., Chadwick, L.R., Nikolic, D., Sun, Y., Cuendet, M.Y., Deng, Y., Hedayat, A.S., Pauli, G.D., Farnsworth, N.R., Breemenvan, R.B., Bolton, J.L., 2005. Comparison of the in vitro estrogenic activities of compounds from hops (*Humulus lupulus*) and red clover (*Trifolium pratense*). J. Agric. Food Chem. 53, 6246–6253.

Overk, C.R., Guo, J., Chadwick, L.R., Lantvit, D.D., Minassi, A., Appendino, G., et al., 2008. In vivo estrogenic comparisons of *Trifolium pratense* (red clover) *Humulus lupulus* (hops), and the pure compounds isoxanthohumol and 8-prenylnaringenin. Chem. Biol. Interact. 176 (1), 30–39.

Paraiso, I.L., Plagmann, L.S., Yang, L., Zielke, R., Gombart, A.F., Maier, C.S., et al., 2019. Reductive metabolism of xanthohumol and 8-prenylnaringenin by the intestinal bacterium *Eubacterium ramulus*. Mol. Nutr. Food Res. 63 (2), e1800923.

Peters, S.A., Jones, C.R., Ungell, A.L., Hatley, O.J., 2016. Predicting drug extraction in the human gut wall: assessing contributions from drug metabolizing enzymes and transporter proteins using preclinical models. Clin. Pharmacokinet. 55 (6), 673–696.

Pinkerton, J.V., 2020. Hormone therapy for postmenopausal women. N. Engl. J. Med. 382 (5), 446–455.

Pohjanvirta, R., Nasri, A., 2022. The potent phytoestrogen 8-prenylnaringenin: a friend or a foe? Int. J. Mol. Sci. 23 (6), 3168.

Possemiers, S., Heyerick, A., Robbens, V., De Keukeleire, D., Verstraete, W., 2005. Activation of proestrogens from hops (*Humulus lupulus L.*) by intestinal microbiota; Conversion of isoxanthohumol into 8-prenylnaringenin. J. Agric. Food Chem. 53 (16), 6281–6288.

Press, B.D.G.D., 2008. Permeability for intestinal absorption: Caco-2 assay and related issues. Curr. Drug Metabol. 9, 893–900.

Punt, A., Pinckaers, N., Peijnenburg, A., Louisse, J., 2021. Development of a web-based toolbox to support quantitative in-vitro-to-in-vivo extrapolations (QIVIVE) within nonanimal testing strategies. Chem. Res. Toxicol. 34 (2), 460–472.

Rietjens, I.M., Sotoca, A.M., Vervoort, J., Louisse, J., 2013. Mechanisms underlying the dualistic mode of action of major soy isoflavones in relation to cell proliferation and cancer risks. Mol. Nutr. Food Res. 57 (1), 100–113.

Rodgers, T., Rowland, M., 2006. Physiologically based pharmacokinetic modelling 2: predicting the tissue distribution of acids, very weak bases, neutrals and zwitterions. J. Pharmaceut. Sci. 95 (6), 1238–1257.

Schaefer, O., Humpel, M., Fritzemeier, K.H., Bohlmann, R., Schleuning, W.D., 2003. 8-Prenylnaringenin is a potent ERalpha selective phytoestrogen present in hops and beer. J. Steroid Biochem. Mol. Biol. 84 (2–3), 359–360.

Sim, K.S., Park, S., Seo, H., Lee, S.H., Lee, H.S., Park, Y., et al., 2022. Comparative study of estrogenic activities of phytoestrogens using OECD in vitro and in vivo testing methods. Toxicol. Appl. Pharmacol. 434, 115815.

Stevens, J.F.T.A., Deinzer, M.L., 1999. Quantitative analysis of xanthohumol and related prenylflavonoids in hops and beer by liquid chromatography-tandem mass spectrometry. J. Chromatogr. A 832 (1–2), 97–107.

Stevens, J.F., Page, J.E., 2004. Xanthohumol and related prenylflavonoids from hops and beer: to your good health. Phytochemistry 65 (10), 1317–1330.

Stevens, J.F., Ivancic, M., Hsu, V.L., Prenylflavonoids, M.L.D., 1997. From humulus lupulus. Phytochemistry 44, 1575–1585.

Sun, D.L.H., Welage, L.S., Barnett, J.L., Landowski, C.P., Foster, D., Fleisher, D., Lee, K. D., Amidon, G.L., 2002. Comparison of human duodenum and Caco-2 gene expression profiles for 12,000 gene sequences tags and correlation with permeability of 26 drugs. Pharmacol. Res. 19, 1400–1416.

Svingen, T., Schwartz, C.L., Rosenmai, A.K., Ramhoj, L., Johansson, H.K.L., Hass, U., et al., 2022. Using alternative test methods to predict endocrine disruption and reproductive adverse outcomes: do we have enough knowledge? Environ. Pollut. 304, 119242.

Teeguarden, J.G., Waechter Jr., J.M., Clewell 3rd, H.J., Covington, T.R., Barton, H.A., 2005. Evaluation of oral and intravenous route pharmacokinetics, plasma protein binding, and uterine tissue dose metrics of bisphenol A: a physiologically based pharmacokinetic approach. Toxicol. Sci. 85 (2), 823–838.

Valentin J. Basic Anatomical and Physiological Data for Use in Radiological Protection Reference Values: ICRP Publication 89. Annals of the ICRP2002.

van Breemen, R.B., Yuan, Y., Banuvar, S., Shulman, L.P., Qiu, X., Alvarenga, R.F., et al., 2014a. Pharmacokinetics of prenylated hop phenols in women following oral administration of a standardized extract of hops. Mol. Nutr. Food Res. 58 (10), 1962–1969.

van Breemen, R.B., Yuan, Y., Banuvar, S., Shulman, L.P., Qiu, X., Alvarenga, R.F., et al., 2014b. Pharmacokinetics of prenylated hop phenols in women following oral administration of a standardized extract of hops. Mol. Nutr. Food Res. 58 (10), 1962–1969.

van Breemen, R.B., Chen, L., Tonsing-Carter, A., Banuvar, S., Barengolts, E., Viana, M., et al., 2020. Pharmacokinetic interactions of a hop dietary supplement with drug metabolism in perimenopausal and postmenopausal women. J. Agric. Food Chem. 68 (18), 5212–5220.

Vesaghhamedani, S., Ebrahimzadeh, F., Najafi, E., Shabgah, O.G., Askari, E., Shabgah, A. G., et al., 2022. Xanthohumol: an underestimated, while potent and promising chemotherapeutic agent in cancer treatment. Prog. Biophys. Mol. Biol. 172, 3–14.

Wang, Y.T., Mohammed, S.D., Farmer, A.D., Wang, D., Zarate, N., Hobson, A.R., et al., 2015. Regional gastrointestinal transit and pH studied in 215 healthy volunteers using the wireless motility capsule: influence of age, gender, study country and testing protocol. Aliment. Pharmacol. Ther. 42 (6), 761–772.

Wang, X., He, B., Shi, J., Li, Q., Zhu, H.J., 2020. Comparative proteomics analysis of human liver microsomes and S9 fractions. Drug Metab. Dispos. 48 (1), 31–40.